euspen's 17th International Conference & Exhibition, Hannover, DE, May 2017
www.euspen.eu

Large stroke three degree-of-freedom spherical flexure joint

M. Naves, R.G.K.M. Aarts, D.M. Brouwer

University of Twente, Enschede, The Netherlands
m.naves@utwente.nl

Abstract
Multi degree of freedom flexure joints are often limited to small deflection angles, because of their strong loss of stiffness in support directions when deflected, or they have a large range of motion but are initially already compliant also in the intended support directions. In this paper, an innovative design for a high performance large stroke spherical flexure joint is presented which can maintain a high level of support stiffness over its full range of motion. A series of flexural topologies are optimized and compared which resulted in a flexure joint design which can achieve a support stiffness of almost 100 N/mm at a tilt angle of 30 degrees. Experimental validations have been conducted in order to validate the results and confirm this high level of support stiffness at large tilt angles.

Keywords: compliant mechanisms, spherical joints, large stroke, flexure mechanisms

1. Introduction

In high precision applications often flexure-based mechanisms are used for their deterministic behaviour. In order to allow for the design of flexure-based spatial manipulators, large stroke spherical flexure joints are often required (e.g. parallel kinematic arrangements). Typical joints often consist of a spherical notch joint or an assembly of blade and wire flexures [1]. However, these type of joints are only suited for minor deflections angles (< 10 degrees), suffer from a lack of support stiffness in load carrying directions (<0.1 N/mm), and the support stiffness decreases strongly with deflection. In this paper a new generic concept for a three degree-of-freedom high performance flexure joint is presented which can attain a high level of support stiffness at large deflection angles. A set of different joint topologies are optimized and compared, and an experimental validation is conducted to verify the results.

2. Conceptual design of the spherical flexure joint

For the design of the spherical flexure joint, a set of folded leafsprings are combined in order to provide support stiffness in the load carrying directions while allowing motion in the desired degrees of freedom. In order to properly constrain the required degrees of freedom, all folded leafspring are oriented such that the folding lines of all folded flexures intersect at a single point, which defines the instant centre of rotation. This concept is schematically illustrated in figure 1a, in which the degrees of freedom are defined as the pan, tip and tilt motion. Furthermore, θ defines the pitch angle of the folded leafspring with respect to the illustrated pan axis. For properly constraining all translational motions, at least three folded leafsprings are required to constrain the three translational degrees of freedom. More folded flexures can be added to potentially improve support stiffness. For clarification, we will subdivide all considered topology variations in three different classifications.

Class 1: Single Stage Spherical joint (S^3)
The most simple topology for a spherical flexure joint is the so-called "single stage spherical joint", where at least three folded leafsprings are directly connected between a fixed world and end-effector. Different variations can be generated by alternating the number of folded leafsprings under a varying pitch angle and by alternating the number of rotational copies around the pan axis. Figure 1a gives an example which includes folded leafsprings under two different pitch angles (*p=2*) copied three times around the pan axis (*c=3*).

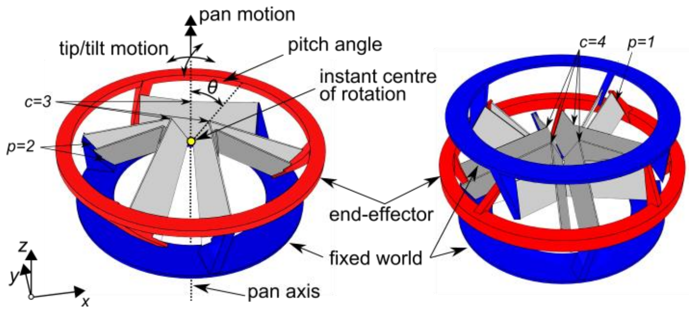

***a:** S^3 joint (p=2, c=3)* ***b**: MS^3 joint (p=1, c=4)*

Figure 1. *Schematic illustration of a S^3 and MS^3 joint*

Class 2: Mirrored Single Stage Spherical joint (MS^3)
The second classification of a valid flexure topology is the so-called "mirrored single stage spherical joint" where two single stage joints are mirrored and merged (and slightly rotated around the pan axis) to increase support in the load carrying directions. Again, different variations can be generated by alternating the number of folded leafsprings. Figure 1b gives an example of a mirrored single stage spherical joint consisting of eight folded leafsprings divided over four circular segments, all under the same pitch angle (*p=1, c=4*).

Class 3: Mirrored Double Stage Spherical joint (MDS^2)
The last classification of flexure topologies is similar to the mirrored single stage spherical joint, except for the difference in attachment to the fixed world. For this classification, the top blue ring (figure 1b) will act as the end-effector instead of a connection to the fixed world. Subsequently, the red ring will operate as an intermediate body. For this class, motion of the joint is divided over the two stages, reducing the extent of the deformations and consequently allowing thicker leafsprings while at similar stress levels.

3. Performance comparison of different topologies

To compare the performance of the different topologies, a shape optimization is used to optimize and compare the support stiffness of a selected set of topologies [2]. This shape optimization is used to obtain the optimal geometrical shape which provides maximum support stiffness for the considered case, where performance is evaluated with the flexible multibody software SPACAR [3]. For this case, we consider a spherical joint which allows for a tip/tilt bidirectional motion of 30 degrees in which pan motion is disregarded. Furthermore, build-space is limited to a cylinder with a radius of 75mm and for material of the leafsprings spring-steel is used where we limit the maximum stress to 300 MPa. As optimization criterion, the vertical support stiffness in co-rotational z-direction at a maximum tilt-angle of 30 degrees is considered. Due to the intertwined nature of the folded leafsprings, collision between flexures over the range of motion plays an essential role during the optimization procedure. By including collision as an extra constraint to be avoided in this optimization, valid joint designs can be assured.

An overview of the attained support stiffness of different optimized topologies in the undeflected and deflected state is given in figure 2. It can be concluded that increasing the number of flexures does not necessarily improve the support stiffness. This is caused by flexure collision where an increment in flexures results in a reduction of the available build-space for each leafspring, potentially reducing the maximum achievable support stiffness. Furthermore, it can be concluded that a secondary mirrored stage of folded leafsprings has a positive effect on the support stiffness, despite the reduction in design freedom due to the increment in flexures. Especially for the double stage topology in which each stage contributes to half of the desired deflection angle (class: MDS^2), the decrease in stiffness when deflected is much less. For the best joint design of the selected topologies, a support stiffness of almost 100 N/mm at 30 degrees deflection is obtained.

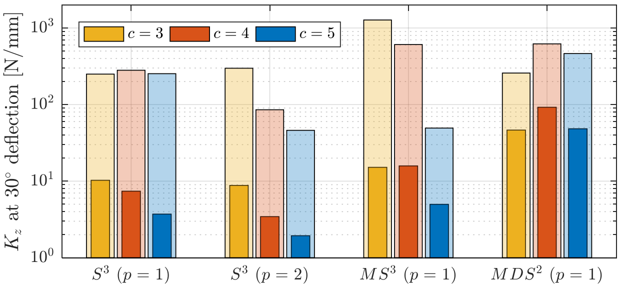

Figure 2. *Support stiffness of the optimized selected set of topologies in deflected state (solid) and undeflected state (transparent) (p: number of folded leafsprings under a varying pitch angle, c: number of rotational copies of folded leafsprings around the pan axis)*

4. Experimental validation

In order to validate the simulations, an experiment is conducted to verify the obtained support stiffness. For this purpose, two spherical joints are manufactured (class: *S^3; p=1, c=3* and class *MDS^2; p=1, c=4*). The joints are manufactured from 3D-printed frame parts of PLA combined with leafsprings made of spring-steel (figure 3). Furthermore, a wire flexure is used to create a bending moment to set the flexure joint in the desired tilt angle. In order to validate simulations, the frequency of the translational eigenmode in the vertical z-direction is evaluated by using the FFT data of three accelerometers placed on the end-effector. As this frequency is directly related to the support stiffness, an assessment can be made of the stiffness in the vertical z-direction. In figure 4, the results from simulations and experiments of both joint designs are displayed. Particularly at small deflection angles, support stiffness appears to be significantly smaller compared to simulations. This deviation can be largely related to limited stiffness of the frame parts which are modelled rigid. Additionally there are manufacturing imperfections, such as a non-zero bending radius, a lack of flatness and alignment errors of the folded leafsprings. As shown previously [4], imperfections in the order of magnitude of a few times the flexure thickness can deteriorate stiffness in some directions in the undeflected state by more than 80%. As expected, with increasing deflection angle, the impact of imperfections reduces and mismatch between experiment and simulations decreases. Despite the difference between experiment and simulations, the relatively high level of support stiffness at maximum deflection angle can be confirmed.

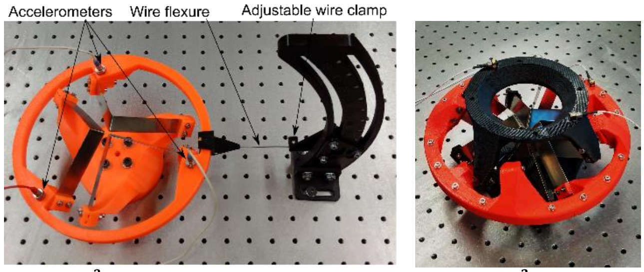

S^3 joint in experimental setup ***MDS^2 joint***

Figure 3. *Experimental setup for validation of support stiffness*

Figure 4. *Experimental validation of the support stiffness of the optimized S^3 and MDS^2 joint*

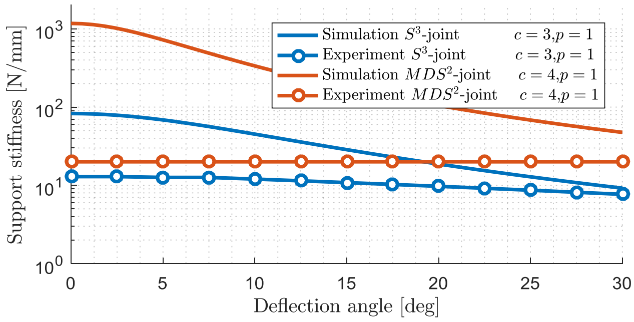

5. Conclusion

By combining a set of folded leafsprings in which the folding line of all leafsprings intersect at a single point, a large range of motion spherical flexure joint is obtained. Structural optimizations on a diverse set of flexure topologies provides insight in suitable flexure designs which provide high support stiffness. For the considered test case concerning a flexure joint which allows for 30 degrees of bidirectional tip/tilt motion, a vertical support stiffness of almost 100 N/mm is obtained at maximum deflection angle, which represents an increase in support stiffness of more than a factor of thousand with respect to traditional spherical flexure joints.

References

[1] Machekposhti D F, Tolou N and Herder J L, 2015, *J. of Mech. Des.* ***137*** *032301*

[2] Naves M, Brouwer D M and Aarts R G K M, 2017, *J. of Mech. and Robotics,* Building block based spatial topology synthesis method for large stroke flexure hinges

[3] Jonker J and Meijaard J, 1990, Spacar --- Computer program for dynamic analysis of flexible spatial mechanisms and manipulators, Multibody systems handbook, Berlin, Heidelberg, Springer Berlin Heidelberg

[4] Meijaard J, 2015, *J. Procedia IUTAM* ***13*** *82-89*